3.2.2 GLI in-water algorithms (OTSK2/5/6/7)

- **Outline of the GLI in-water algorithm**

GLI ocean algorithms are listed below (Table A1). Summary table and algorithms flow chart of the GLI in-water algorithms are shown in Table A2 and Figure A1.

Table A1 GLI ocean algorithms

Algorithm code	target	Investigator
Standard algorithms (Dec 2003)		
OTSK1	Atmospheric correction	Fukushima, Frouin
OTSK2	Chlorophyll-a concentration	Mitchell
OTSK5	Attenuation at 490nm	Mitchell
OTSK6	Suspended solid concentration	Kishino
OTSK7	Colored dissolved organic matter	Mitchell
OTSK14	Photosynthetically available radiation	Frouin
OTSK13	Bulk sea surface temperature	Kawamura
Research algorithms		
OTSK3	Accessory pigment (Carotenoid, Phycobilin)	
OTSK4a	Primary production by ecosystem model	
OTSK4b	Primary production by natural fluorescence	
OTSK8	In-water optical measurements	
OTSK9	Study of in-water optical parameters	
OTSK10	Measurements for atmospheric correction	
OTSK11	In-situ SST measurements	
OTSK12	Vicarious calibration measurements	
OTSK16	Skin sea surface temperature	
OTSK17	Phytoplankton species (Trichodesmium)	
OTSK18	Phytoplankton species (Coccolithus)	
OTSK19	AP and APH	

Table A2. Formulations of the GLI in-water algorithms

Variable	Algorithm source	Type	Equation, Coefficients (a), Band Ratio (R)
CHLA	OC4-GLIv3 Modified from O'Reilly et al., 1998	Max Band Ratio, Modified Cubic Polynomial	CHLA = $10^{(a0 + a1*R + a2*R^2 + a3*R^3) + a4}$
			a=[0.531, –3.559,4.488, –2.169, –0.230]
			R = $\log_{10}$(NWLR443 > NWLR460 > NWLR520) / NLWR545)
K490	GLI-K490 Modified from Mitchell and Kahru, 1998	Cubic polynomial in log-log	K490 = $10^{(a0 + a1*R + a2*R^2 + a3*R^3)}$
			a=[–0.825, –1.362, 1.094, –0.777]
			R = $\log_{10}$(NWLR460/NLWR545)
CDOM	In preparation	Linear band ratio in log-log	CDOM440 = $10^{(a0 + a1*R)}$
			a = [–1.493, –1.618]
			R = $\log_{10}$(NWLR443/NLWR520)
REDTIDE	Kahru and Mitchell, 1998	Threshold of band ratio	REDTIDE index > 0, if R < 0.8 and CHLA (1.0
			R = NWLR380/NLWR412
PIGMENT	O'Reilly et al., 1998	Power function	PIGMENT = $1.34*CHLA^{0.98}$

CAROT	Derived from Aiken et al., 1998	Linear regression	CAROT = 0.135 + 0.912*CHLA
SS	Kishino	Neural network	SS=IOSS+OSS IOSS←Neural network OSS=10^(0.074*($\log_{10}$(CHLA))^2+0.8411*$\log_{10}$(CHLA) −0.3273)
Turbid Case2 water	Park	Threshold of NLWR545	Turbid case 2 water flag =1, if NWLR545 > threshold
			Threshold is determined with CHLA (see text)

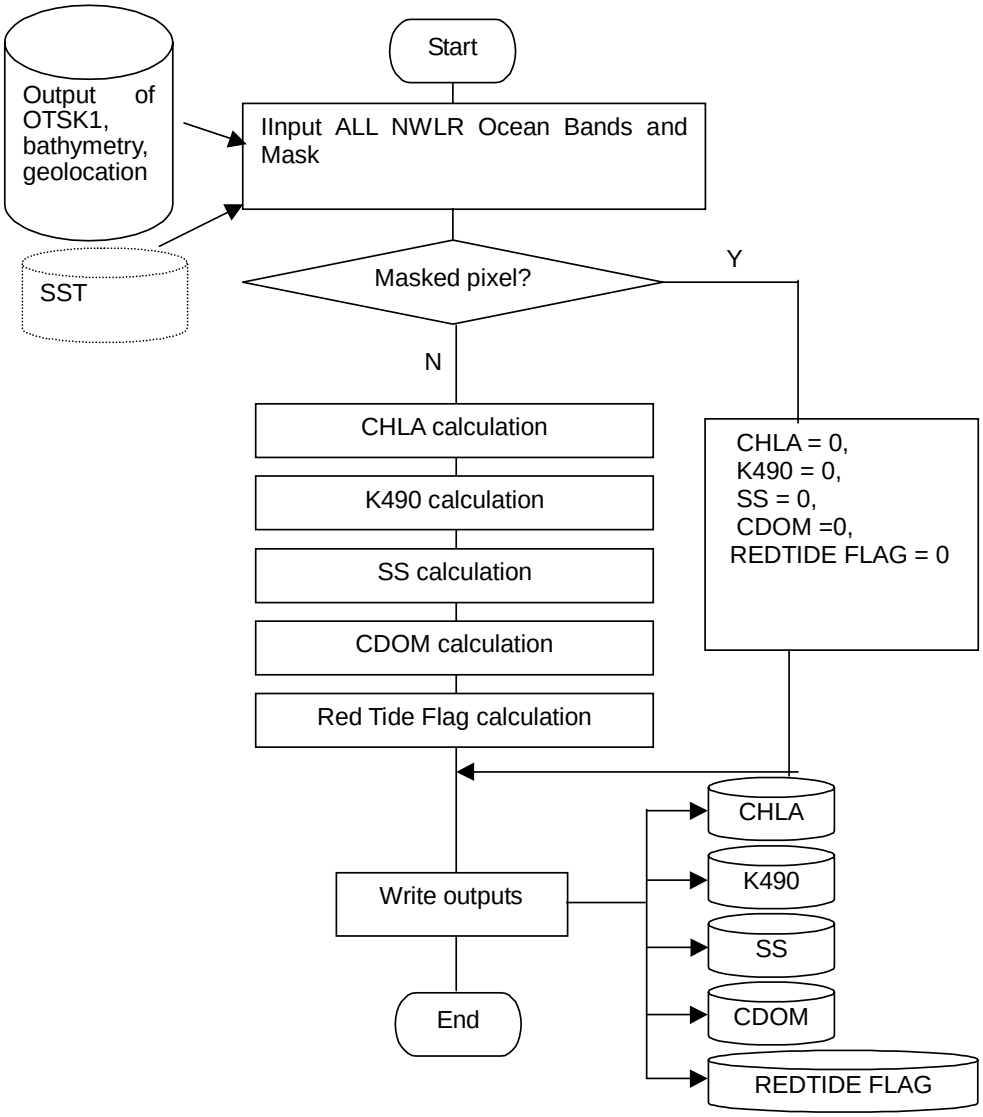

Figure A1. Algorithm flow chart of OTSK2, 5, 6 and 7

• Chlorophyll-a, colored dissolved organic matter, and K490 algorithms (OTSK2/6/7)

A. Algorithm Outline

(1) Algorithm Code: OTSK2, 5, 7, 3, 4a/b, 8, 9

(2) Product Code: CHLA, K490, CDOM (Status: standard level), CAROT (Status: Research level)

(3) PI names: G-0020 B.Greg Mitchell for OTSK2,5,7

(4) Overview of algorithm

The goals of this project are to develop algorithms for GLI using our large, global bio-optical database (including CalCOFI, Indian Ocean, sub-tropical Atlantic Ocean, Western Pacific, Japan Sea, East China Sea, Southern Ocean, and ACE-Asia). Other regional and global bio-optical data sets will be merged with our database. Our bio-optical data set includes spectral reflectance (various channels depending on the instrument), pigments (fluorometric and HPLC) and absorption coefficients for particulate and soluble material. Our current database includes more than 1000 high-quality sets of reflectance and chlorophyll data in non-polar oceans areas and over 100 data points from the Southern Ocean. Including multiple casts per station the total number of radiometric profiles is over 3500. Our radiometric data does not have exact spectral band center and bandwidth match for all the GLI ocean color bands. Therefore, we use spline interpolation to estimate remote sensing reflectance (Rrs) at any wavelength and then convert Rrs to normalized water leaving radiances (NWLR) at GLI bands using F_0bar weighted over the response function of each GLI band. In the future we may use optical models to generate high spectral resolution synthesis of our actual observations and estimate NWLR in the GLI bands from these models but at present the spline interpolation procedure seems to be sufficiently accurate considering other sources of errors and the widths of the GLI bands. We present our current versions of GLI standard algorithms for chlorophyll, pigments, K490, CDOM and red tide detection. Our preliminary semi-analytical algorithm is capable of deriving CHLA, CDOM, spectral absorption and backscattering coefficients for particulate matter but needs refinement as it is currently inferior to empirical algorithms for standard products.

B. Theoretical Description

(1) Methodology and Logic flow

As discussed elsewhere (Mitchell and Kahru 1998, O'Reilly et al. 1998, Kahru and Mitchell 1999), simple 2-band empirical algorithms perform well in Case 1 waters for deriving standard products of CHLA and K490 and a novel indicator of red tides. Our preliminary version of a semianalytic algorithm as well as other semianalytic algorithms (Garver and Siegel 1997, Carder et al. 1999) are capable of deriving more products (e.g. the spectral absorption and backscattering coefficients) but due to atmospheric correction uncertainty at short wavelengths and parameterization problems they are currently inferior to empirical algorithms for standard products.

Our previous CHLA algorithm was based on the CAL-P6 algorithm (Kahru and Mitchell 1999) and used NWLR490/NWLR565. Due to the possible saturation problem at both of these bends we changed the CHLA algorithm during 2000. Our analysis shows that normalizing to NWLR545 may actually improve CHLA retrieval compared to normalizing to NWLR565. The GLI NWLR545 does not have the saturation problem either. Among the band ratios with NWLR545 the sequence of preference is as follows: NWLR490, NWLR460, NWLR443. Unfortunately we cannot use the best band ratio NWLR490/NWLR545 (see Table 1) due to the saturation problem at the GLI 490 nm band. Our second choice is a maximum band ratio (MBR) algorithm

using 3 bands (the maximum of NWLR443, NWLR460 and NWLR520) with NWLR545 in the denominator. This MBR algorithm is slightly superior to other band ratio algorithms not using NWLR490. In satellite-derived NWLR data the use of MBR has additional advantages. A well-known problem with the SeaWiFS ocean color sensor is the underestimation of NWLR at shorter wavelengths that is quite drastic at 412 nm but commonly evident even at 443 nm. As the MBR algorithm picks the maximum ratio, it will reduce the effects of biased NWLR by switching to longer wavelengths in such a case. The MBR concept was introduced by O'Reilly et al. (1998) and applies a single set of coefficients to a band ratio selected as maximum among a set of band ratios. The band actually used in the numerator changes from shorter wavelengths to longer wavelengths with increase in CHLA. We modified the scheme of O'Reilly et al. (1998) by selecting the maximum among the NWLR ratios and not Rrs ratios. This improves CHLA retrieval significantly as it shifts the actually used band towards longer wavelengths with better correlation with CHLA. The algorithm covers the full range of CHLA from 0.01 to 100. This report provides updated coefficients in Table 2 based on work in 2001 to merge new data sets.

Table 1. Comparison of different CHLA algorithms using modified cubic polynomial formulation $CHLA = 10^{(a0 + a1*R + a2*R^2 + a3*R^3)} + a4$. Due to the saturation problem of NWLR490 we are currently recommending to use algorithm 3 with the coefficients in Table A2.

	Band Ratio	R^2	RMS Error
1	$R = \log_{10}(NWLR490 / NWLR545)$	0.944	0.1217
2	$R = \log_{10}((NWLR443 > NWLR460 > NWLR520) / NWLR545)$	0.941	0.1249
3	$R = \log_{10}((NWLR443 > NWLR460 > NWLR520) / NWLR545)$	0.938	0.1270

In March 2002 the K490 algorithm was modified from our previous version due to the possible saturation problem of the GLI 490 and 565 bands. The current K490 product is derived as a cubic function of NWLR460/NWLR545 in the log-log space (Table 2, Fig. 3). It provides better retrieval compared to the original approach of SeaWiFS using NWLR443/NWLR555. Due to measurement error in the K490 estimates in very clear waters, some K490 estimates that were below the estimated pure water values were excluded in the coefficient optimization.

As we have previously reported (Mitchell and Holm-Hansen, 1991; Mitchell 1992), the Southern Ocean has significantly different bio-optical relationships compared to lower latitudes. Figure 4 shows our SPG ANT MBR algorithm fitted to our updated JGOFS and AMLR data sets compared to the standard NASA OC4v4 (note at this time SPG ANT is for SeaWiFS wavelengths, not GLI alternative bands). Figure 5 shows the error of the NASA OC4v4 as a function of CHL concentration. In the range of 0.2 – 2.0 mg m^{-3}, OC4v4 will underestimate CHL in the Southern Ocean by about 30-50%. This is the range of CHL that predominates in the Southern Ocean and therefore it is essential to determine alternative algorithms for these regions. In Figure 6 we show match ups for CHL between ship surveys and SeaWiFS. The underestimates that are indicated in our in situ algorithm data set (Figure 4) indeed are confirmed in the satellite - ship comparison of Figure 6 underscoring a need to resolve the issues related to Southern Ocean algorithms. We note that there should also be special attention to Arctic algorithms (Mitchell 1992) but we do not have data with new instruments to confirm our early observations.

For the CDOM product all combinations of GLI band ratios were tested versus *in situ* measurements of $a_s(300)$, i.e. absorption coefficient of dissolved material at 300 nm. Several band ratios provided similar values of r^2 and RMS error. The best band ratio with the highest r^2 and lowest RMSE appeared to be NLWN380/NWLN545 (r^2 = 0.802, RMSE = 0.059). Band ratios NLWN412/NWLN520, NLWN412/NWLN545 and NLWN443/NWLN520 were slightly but not significantly inferior. A large proportion of the scatter is actually due to measurement errors and not due to algorithm errors. Our experience with SeaWiFS (Kahru and Mitchell 1999) shows that atmospheric correction at short wavelengths in the coastal zone may have large errors. Therefore we did not select band ratios including short wavelength bands (380, 412 nm) for the CDOM algorithm. As similar results can be achieved with other bands for which atmospheric correction should be more robust, we selected NWLR443/NWLN520. This ratio appears to be well correlated with CDOM absorption due to the fact that a significant part of phytoplankton influence on this ratio tends to cancel out. Additional advantage of this band ratio (compared to band ratios using bands 380 and 400 nm) is that 443 and 520 nm bands are common on other sensors and the same algorithm can therefore be used on these sensors, provided that accurate NWLR values are available. The operational CDOM definition is the amount of absorption by the dissolved organic component at a certain wavelength. We originally used the wavelength of $a_s(300)$ as a proxy to the concentration of CDOM due to a better signal to noise ratio at this wavelength. At 440 nm wavelength the relative amount of measurement error is significantly higher which results in the reduction in r^2 of the estimate. Per request of Dr. Kishino and according to original NASDA plans, we are now providing algorithm for $a_s(440)$.

A novel algorithm for the detection of red tides has been developed using the unique 380 nm spectral band available on GLI that is not available on other planned ocean color satellites. The algorithm is based on the approach described in Kahru and Mitchell (1998) and should allow detection of blooms of common red tide organisms with high intracellular concentrations of mycosporin-like amino acids (MAAs). For chlorophyll concentrations greater than 1-2 mg m^{-3} the ratio NWLR380/NWLR412 diverges significantly for the red tide data set compared to comparable chlorophyll concentrations observed for routine CalCOFI cruises. The availability of the 380 nm band on GLI allows the potential for red tide detection while concentrations are still moderate. It is critical for this algorithm that the NWLR380 and NWLR412 values are accurately derived. This may not be an easy task considering the problems with SeaWiFS at 412 and 443 nm (Kahru and Mitchell 1999).

(2) Physical and Mathematical aspects of the algorithm

The algorithms are simple, empirical relationships based on in-water NWLR and measurements of the products of interest. There are no physical assumptions and the equations are derived from the best fits of measurements with a few constraints.

C. Practical Considerations

(1) Programming, Procedural, Running Considerations

Program Requirements: Table 2 shows information about the expected software generated from this algorithm

Table 2.

Program Memory	N/A
Program Size	Each algorithm less than 100 lines of C code
Required Channels	All GLI Ocean Bands
Necessary/Ancillary Data	Top-of-Atmosphere radiances in bands with saturation problem, SST, Bathymetry, Geo-location (latitude, longitude)

Expected Disk Volume	2 bytes per pixel per algorithm per product
Special Programs or Subroutines	NONE

D. Publications and Papers

1. Kahru, M. and B.G. Mitchell, *Bio-optics and remote sensing of a massive red tide off Southern California*, ASLO Aquatic Sciences Meeting, Santa Fe, New Mexico, February 10-14, 1997, p.203-204.
2. Kahru, M., and B.G. Mitchell, 1998, Spectral reflectance and absorption of a massive red tide off southern California, *Journal of Geophysical Research*, **103**(C), 21601-21610, 1998.
3. Mitchell, B.G. and M. Kahru, Algorithms for SeaWiFS standard products developed with the CalCOFI bio-optical data set, *Cal. Coop. Ocean. Fish. Invest. R.*, 39:133-147, 1998.
4. O'Reilly, J.E., S. Maritorena, B.G. Mitchell, D.A. Siegel, K.L. Carder, S.A. Garver, M. Kahru, and C.R. McClain, Ocean color chlorophyll algorithms for SeaWiFS, *J. Geophys. Res.*, 103(C):24,937-24,953, 1998.
5. Kahru, M. and B. G. Mitchell. Empirical chlorophyll algorithm and preliminary SeaWiFS validation for the California Current, Int. J. of Remote Sensing, 20: 3423-3429, 1999.
6. Kahru, M., B.G. Mitchell. Influence of the 1997-98 El Niño on the surface chlorophyll in the California Current, Geophysical Research Letters, Vol. 27, No. 18, 2937-2940, 2000.
7. Kahru, M. and B. G. Mitchell. Seasonal and non-seasonal variability of satellite-derived chlorophyll and CDOM concentration in the California Current. J. Geophys. Res, 106(C2): 2517, 2001.

E. References

1. Aiken, J., G.F. Moore, C.C. Trees, S.B. Hooker, and D.K. Clark, The SeaWiFS CZCS-type pigment algorithm, NASA Tech. Memo. 104566, vol. 29, 34 pp., 1995.
2. Carder, K.L, F.R. Chen, Z.P. Lee, and S.K. Hawes, Semianalytic Moderate-Resolution Imaging Spectrometer algorithms for chlorophyll a and absorption with bio-optical domains based on nitrate-depletion temperatures. *J. Geophys. Res*., 104(C3):5403-5421, 1999.
3. Garver, S.A., and D.A. Siegel, Inherent optical property inversion of ocean color spectra and its biogeochemical interpretation. 1. Time series from the Sargasso Sea. *J. Geophys. Res*., 102(C8):18,607-18,625, 1997.
4. Kahru, M., and B.G. Mitchell, Spectral reflectance and absorption of a massive red tide off southern California, *Journal of Geophysical Research*, **103**(C), 21601-21610, 1998.
5. Mitchell, B.G. and M. Kahru, Algorithms for SeaWiFS standard products developed with the CalCOFI bio-optical data set, *Cal. Coop. Ocean. Fish. Invest. R.*, 39:133-147, 1998.
6. O'Reilly, J.E., S. Maritorena, B.G. Mitchell, D.A. Siegel, K.L. Carder, S.A. Garver, M. Kahru, and C.R. McClain, Ocean color chlorophyll algorithms for SeaWiFS, *J. Geophys. Res.*, 103(C):24,937-24,953, 1998.
7. Kahru, M. and B. G. Mitchell. Empirical chlorophyll algorithm and preliminary SeaWiFS validation for the California Current, Int. J. of Remote Sensing, in press, 1999.

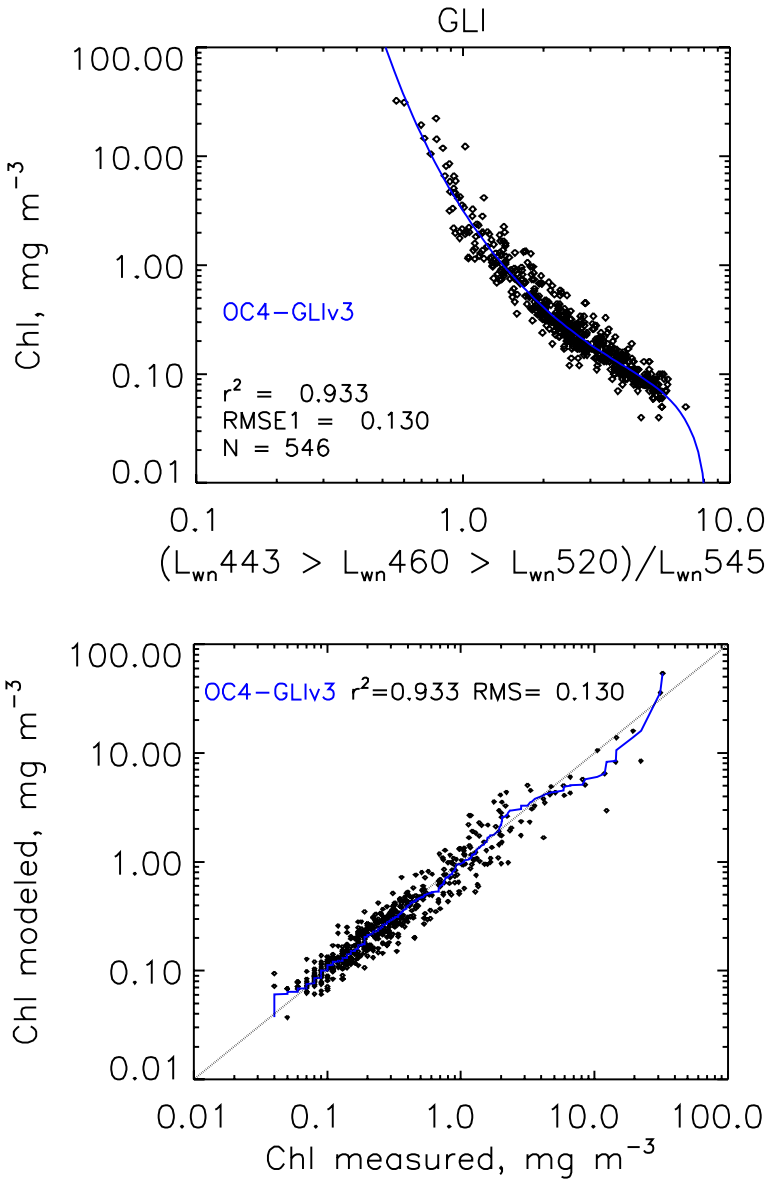

Figure 1. Top, GLI CHLA algorithm (OC4-GLI version 3) using the maximum band ratio of NWLR443, NWLR460, NWLR520 to NWLR545 shown as the blue line. Symbols are the non-polar algorithm data set used for the fitting. Bottom, Ship-measured chl compared to OC4 GLIv3 estimate of chl for our algorithm data set.

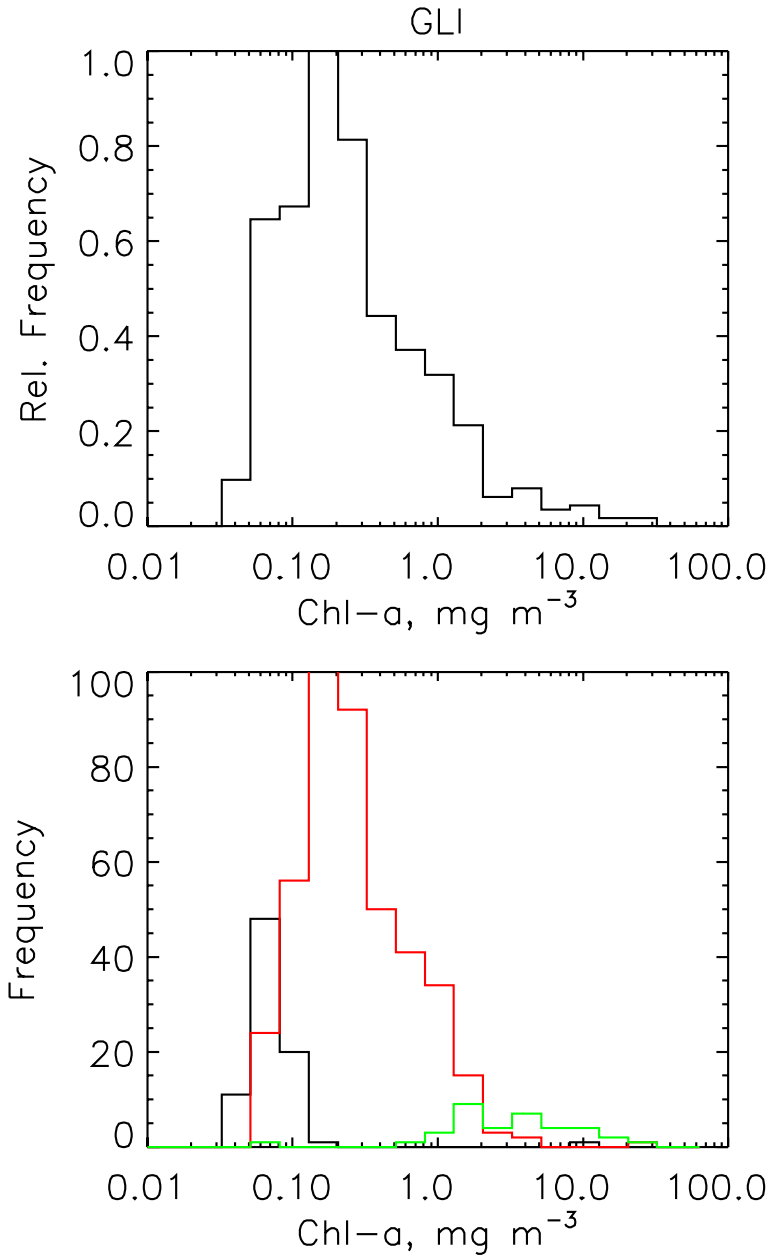

Figure 2. Distribution histogram of CHLA in the bio-optical database (top) and the switching of bands used in the maximum-band-ratio algorithm OC4-GLI (bottom). The distribution histograms are shown for NWLR443 (black), NWLR460 (red) and NWLR520 (green) as a function of CHLA. NWLR443 is used at low CHLA, NWLR460 in the middle range and NWLR520 at high CHLA.

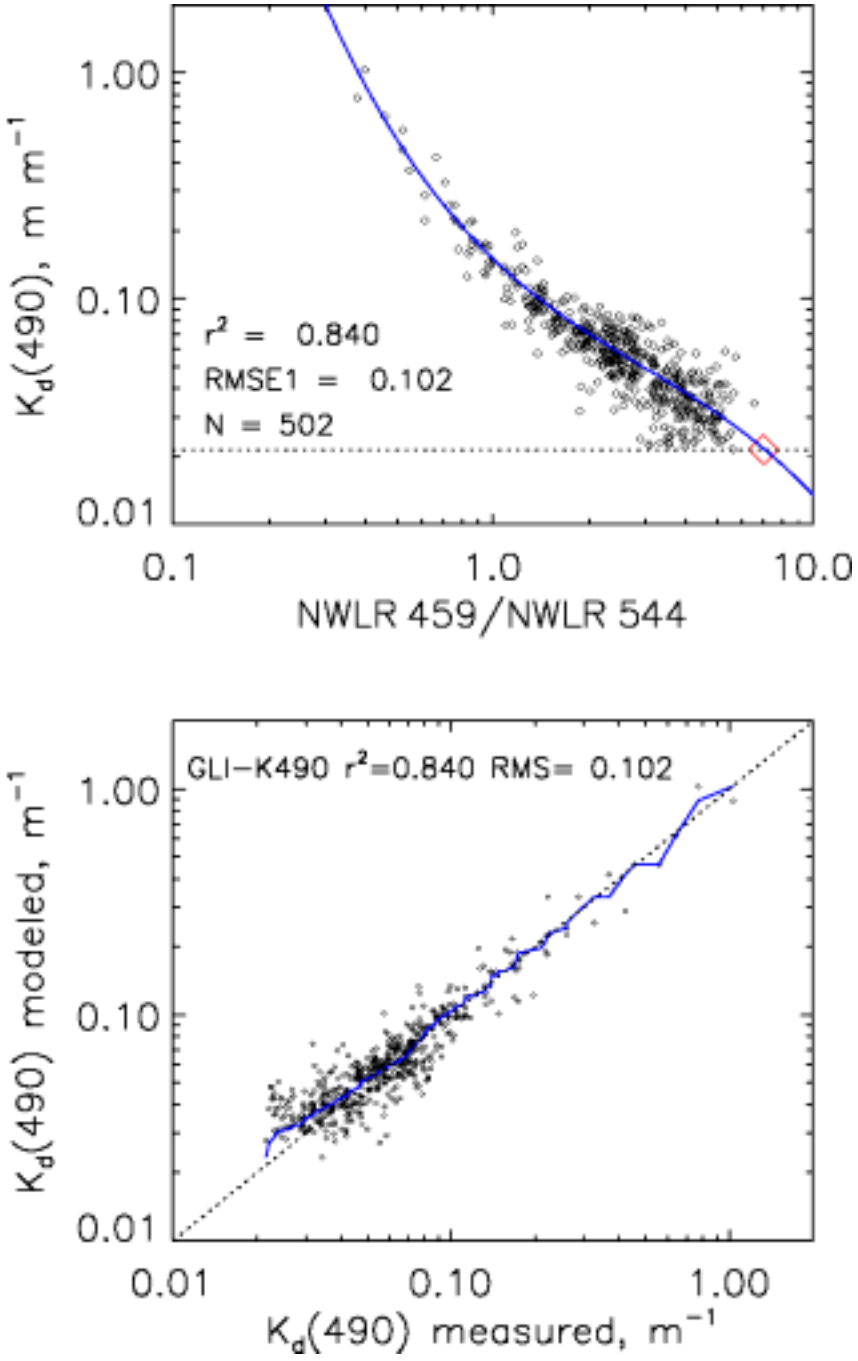

Figure 3. The GLI K490 algorithm using band ratio of NWLR460 and NWLR545 (top). The pure water value is shown with a horizontal dashed line, estimated pure water reflectance and K490 are shown as a big red diamond. The quantile-quantile plot is shown in bottom panel.

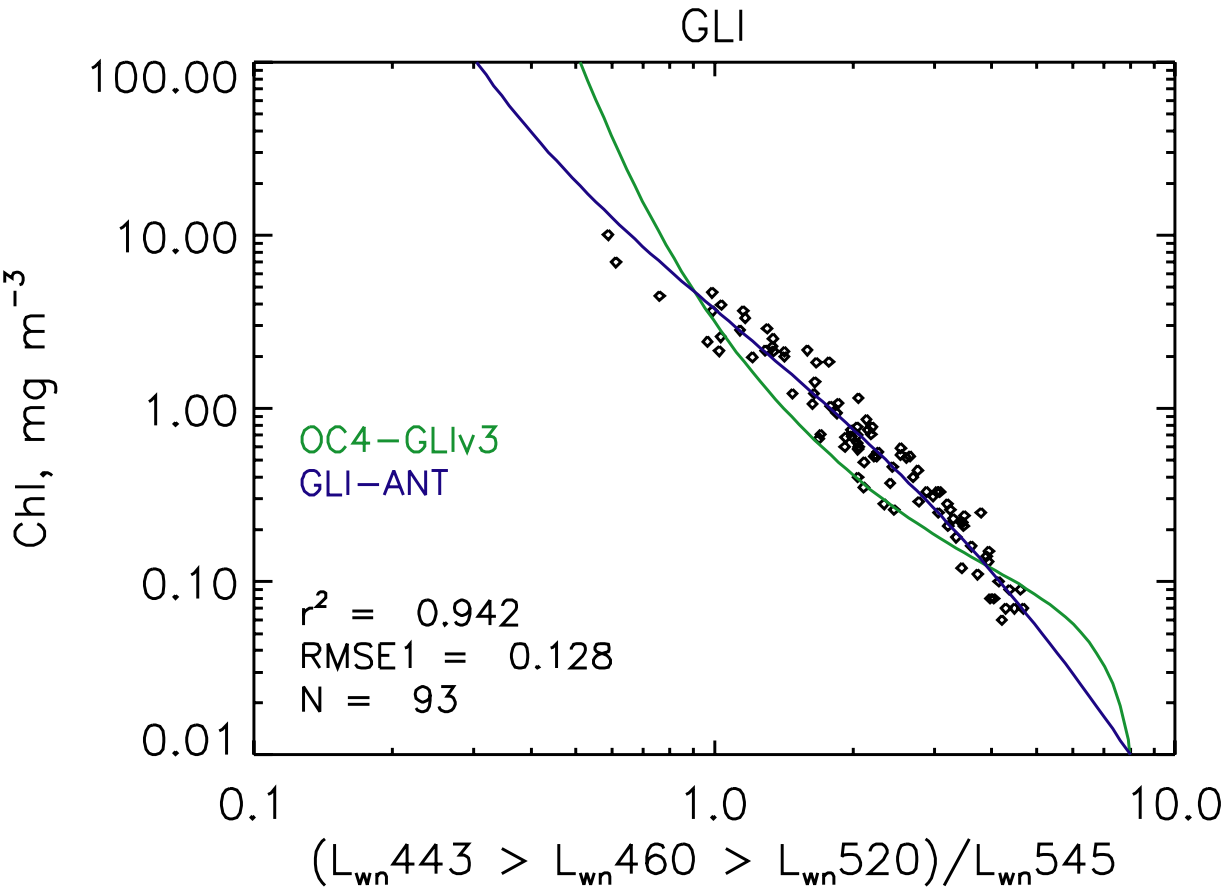

Figure 4. GLI Southern Ocean CHLA algorithm (GLI-ANT) using the maximum band ratio of NWLR443, NWLR460, NWLR520 to NWLR545 (blue line) compared to current global GLI CHLA algorithm OC4-GLIv3 (green line).

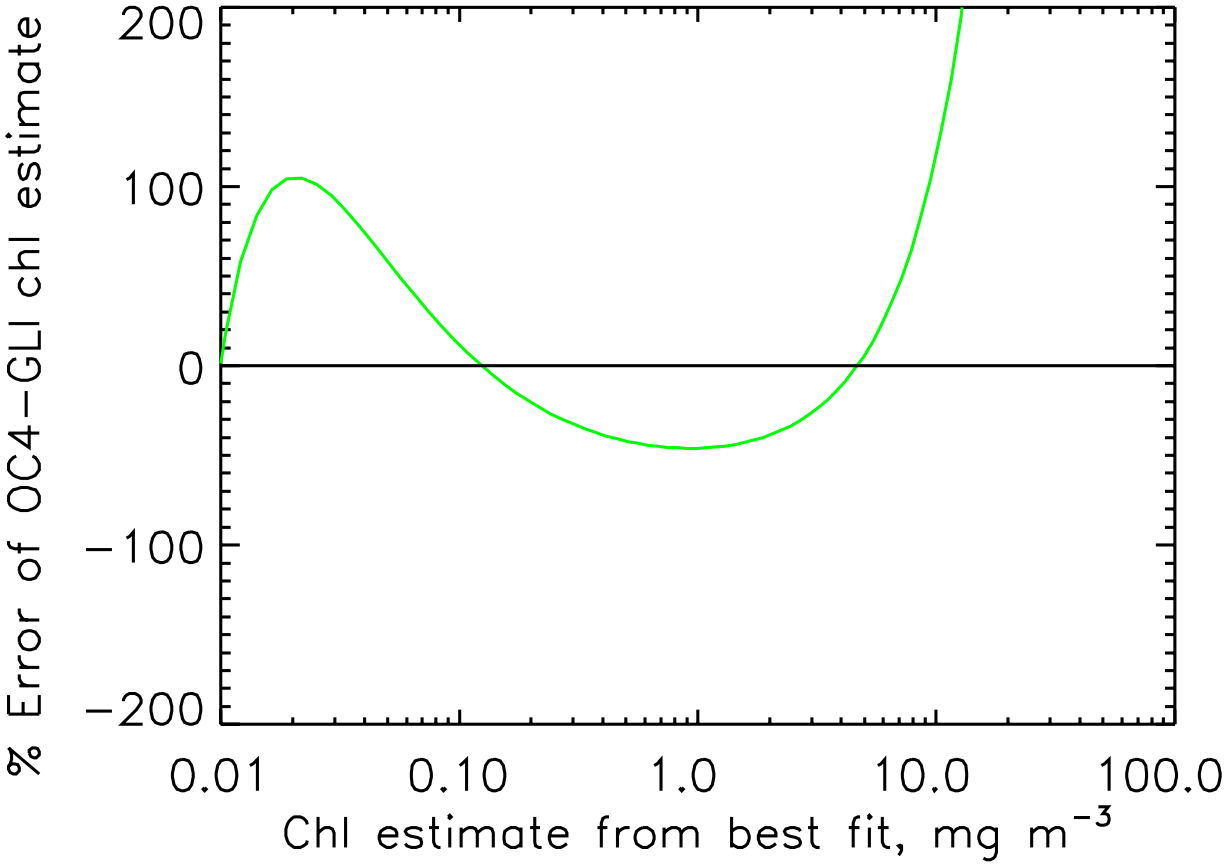

Figure 5. Percent error that results from using the current GLI CHLA algorithm OC4-GLIv3 compared to GLI-ANT. The OC4-GLIv3 algorithm would underestimate CHLA at moderate concentrations (from about 0.1 to 5 mg m-3) but would overestimate at both low and high concentrations.

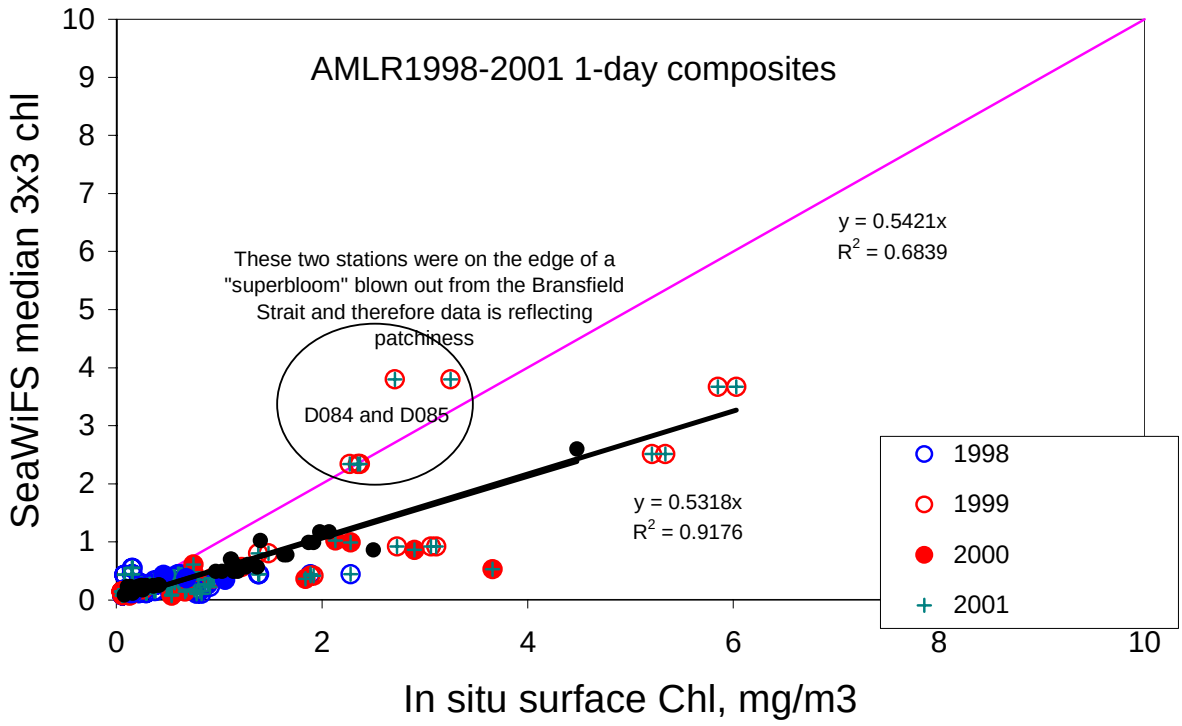

Figure 6. Evidence for the underestimation by SeaWiFS of Southern Ocean CHLA at medium CHLA concentration. As evidenced by the slope of the regression, the OC4v4 algorithm shows only 54% of in situ CHLA. Evidence for the possible overestimation at very low CHLA is not conclusive but possible.

• Suspended solid algorithm (OTSK6)

A. Algorithm Outline

(1) Algorithm Code: OTSK6

(2) Product Code: SS (Status: standard level)

(3) PI names: G-0059 Motoaki Kishino for OTSK6

B. Theoretical Description

(1) introduction

The substances that determine the turbidity of the ocean are phytoplankton, its degradation organic matter (suspended or dissolved), and inorganic suspended matter such as clay particles. In general, in open oceans, phytoplankton and organic matter exist but inorganic matter does not in most cases (Case 1 waters). However, in coastal waters, a lot of organic and inorganic suspended matter is transported by river from land. Eutrophication of water also occurs by land-originated nutrient, which brings phytoplankton bloom and sometimes red tide. Under this condition, light distribution is quite different from that in open oceans (Case 2 waters).

Traditional chlorophyll algorithm developed for case 1 waters gives in many cases too high value of chlorophyll if applied to coastal waters. In open oceans, phytoplankton and its byproducts control the radiation transfer, and the data (remote sensing reflectance, or normalized water leaving radiance) after atmospheric correction of satellite ocean color shows the spectra that is determined almost by chlorophyll concentration. On the contrary, in coastal waters, dissolved organic matter or suspended inorganic matter affect the underwater light field. Therefore, the traditional algorithms that do not take into account this effect cause significant error since they tend to attribute the spectra entirely to chlorophyll concentration.

Ocean color algorithm for coastal zone need to be constructed taking into account all of phytoplankton, organic or inorganic suspended matter and dissolved organic matter. It is extremely difficult to use traditional empirical method (e.g. band ratio) for that purpose. The concentration of various materials should be considered. As a candidate, there is inversion method that inverses remote sensing reflectance or normalize water leaving radiance. In inversion technique are the direct solution, the matrix inversion technique and so on. However, its disadvantage is to take significant time to find solution. While neural network needs time to be educated, it can process data within a short period.

(2) Database

Ocean color database obtained by Japanese scientists includes in-water radiance, chlorophyll concentration and so on, measured by the groups from Hokkaido University, Tokyo University of Fisheries, National Polar Research Institute, RIKEN, Tokai University, Nagasaki University and local Fisheries Institutes. This database covers wide area from Bering Sea in the north to Southern Ocean in the south, and includes a lot of data from near-Japan seas, coastal waters and inland waters. But the number of suspended solid data is very limited.

In this study, the database was built from the data measured by Tokyo University of Fisheries, National Polar Research Institute, RIKEN and Nagasaki University. The total data were 306. PRR-600, MER-2040, PRR-800 (Biospherical Inc.) were used to measure in-water radiance/irradiance. When the instrument does not include any GLI band, interpolation was performed as follows.

1) For PRR-800 data, the target band was estimated from several bands in both sides by Spline interpolation.

400 nm: interpolated using 4 bands, 380 nm, 395 nm, 412 nm, 443 nm

460 nm: interpolated using 4 bands, 412 nm, 443 nm, 465 nm, 490 nm

545 nm: interpolated using 4 bands, 520 nm, 532 nm, 555 nm, 565 nm

2) In other cases, the target band was obtained using the relationship between interpolated value and four bands

3) When one band of nearest two bands does not exist, the relationship of the two bands is obtained from the data of two bands that measured at the same time (Interpolation (Rrs)-2 in Original.xls)

520 nm: from 510 nm

565 nm: from 555 nm

From the database, the relationship between chlorophyll-a concentration and suspended solid was found. In Case 1 waters, a certain relationship probably exists between two parameters. First, we removed the data of extremely small SS concentration, which may come from measurement error. Second, we also excluded the data of extremely high SS concentration compared to other measurements with nearly same chlorophyll concentration, because it may include significant amount of inorganic SS. As a result, we found the relationship between chlorophyll concentration and SS concentration (Fig.SS-1). After such data quality control, 74 data remained. These data can be considered those measured in Case 1 waters.

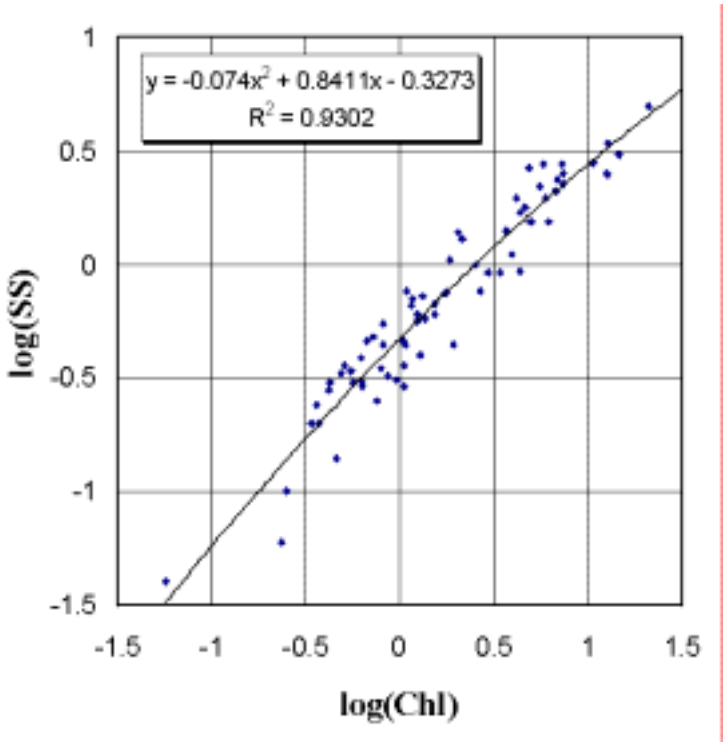

Figure SS-1 The relationship between chlorophyll *a* (Chl) and suspended solid (SS) concentrations.

Black line shows regression line.

SS= 10^(-0.074($\log_{10}$(Chl))^2 + 0.8411($\log_{10}$(Chl))-0.3273) r =0.930

(3) Algorithm

SS can be split into organic suspended solid (OSS) and inorganic suspended solid (IOSS).

The OSS can be estimated using chlorophyll *a* concentration (Fig. SS-1). To estimate IOSS, an neural network (NN) algorithm which inversed bio-optical model was developed. The bio-optical model based on Joseph's two-stream equations (Joseph, 1950) is to simulate remote sensing reflectance (Rrs) at 412, 443, 460, 520 and 545nm from concentrations of chlorophyll a, IOSS and CDOM. Although the Joseph's two-stream equation includes assumptions such as it is realized under the total diffuse light, advantage of using the equation can be expressed by two parameters that are absorption coefficient and backscattering coefficient. Using the Joseph's two-stream equation, Doerffer (1979) shows a good result from a laboratory experiment.

The NN algorithm require a education in order to determine biases of each neuron and weight among neurons. To make data set for education of the NN, 100,000 pairs of Rrs at 412, 443, 460, 520 and 545nm were simulated by bio-optical model from random concentrations of chlorophyll a, IOSS and CDOM, respectively. The Stuttgart Neural Network Simulator (SNNS) was used for the NN construction and education.

A result of the NN algorithm applied to in situ data is shown in Fig. SS-2. We propose the NN algorithm shown in the figure to be the algorithm for SS.

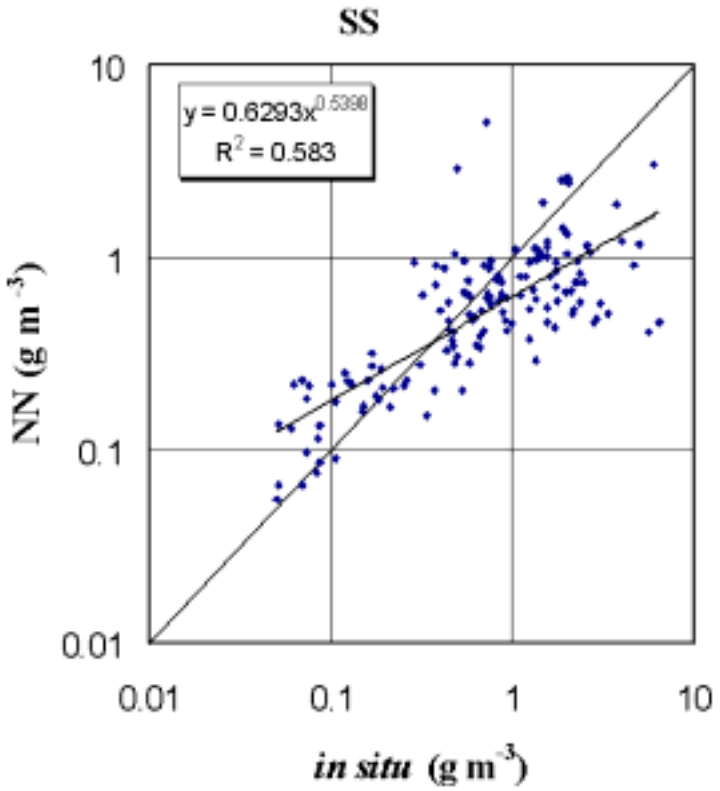

Figure SS-2 Relation between *in situ* data and retrieved by neural network (NN)

(4) Conclusion in this subsection

SS concentration measurements may include considerable error from the spots in suspended solid itself and the foreign dusts, which differs from other measurements. As a result, the correlation is not so high. Algorithm should be improved with more truth data in future.

For Case 2 waters, with the advanced model of optical process, the algorithm for estimating both SS and dissolved organic matter should be established. For that purpose, the optical property measurement of various

materials, the establishment of the relationship of optical property and in-water materials in various ocean areas are required.

D. References

1. Doerffer, R., Application of a two-flow model for remote sensing of substances in water, Boundary-Layer Meteol., vol. 18, 221-232, 1979.
2. Joseph, J., Untersuchungen über Ober- und Unterlichtmessungen im Meere und über ihren Zusammenhang mit Durchsichtigkeitsmessungen, Deut. Hydorograph. Z., vol. 3, 324-335, 1950.

- **Turbid Case 2 water flag algorithm**

A. Algorithm Outline

(1) Algorithm Code: OTSK9

(2) Product Code: *flag*

(3) PI names: *(Y. J. Park, JAXA)*

B. Theoretical Description

Turbid case 2 water flag will be set on for the pixels of which water reflectance is greater than case 1 water limit. In general, water reflectance varies with chlorophyll and other substance in water. But, to minimize the absorption effect of colored dissolved organic matter and chlorophyll, green or red band is chosen for this flag. For GLI, 545nm band will be used, since 565 nm band that planned to use can be easily saturated for turbid pixels.

In this description, we use a simple model of water reflectance, R (A. Morel, JGR, 1988):

$$R = 0.33 \cdot \frac{b_b}{a}, \quad (1)$$

where a, b_b are absorption and backscattering coefficient. There is another relationship between absorption and reflectance in case 1 waters (A. Morel, JGR, 1988):

$$a = \frac{0.9 \cdot K \cdot (1-R)}{1+2.25 \cdot R}, \quad (2)$$

where K is diffuse attenuation coefficient.

From these equations, we can get an expression of R as a function of K and b_b:

$$R = \left((1-2.25 \cdot B) - \sqrt{(1-2.25 \cdot B)^2 - 4B} \right) / 2, \quad (3)$$

where $B \equiv \frac{0.33 b_b}{0.9K}$.

So, we can compute water reflectance for case 1 waters if we know b_b and K, both of which are determined by chlorophyll concentration for case 1 waters. Note that we can use absorption coefficient directly than diffuse attenuation coefficient, K. However, taking into consideration that K model (that is built from insitu measurements) is more reliable than a for the present time (Morel and Maritorena, JGR 106, 2001), we use K rather than a.

Recent update of models for K and b_b (Morel and Maritorena, JGR 106, 2001) shows

$$K(545nm) = 0.05212 + 0.04253 \cdot [chl]^{0.656}, \text{ at 545 nm.} \quad (4)$$

$$b_b(545nm) = 0.0010 + (0.002 + 0.01\,(0.5 - 0.25 \log_{10}[chl])\,(550/545)\, b_p(550) \quad (5)$$

where $b_p(550) = 0.416 \cdot [chl]^{0.766}$.

In the expression of b_b, we don't consider the variation of spectral dependence with chlorophyll concentration because 545nm and 555nm are very close so that the effect is minor in computing b_b at 545. We assume that the upper limit of particle scattering in case 1 water is 1.5 times (threshold factor) of average model:

$$B_{p,lim}(550) = 0.416\,[chl]^{0.766} \times 3.5 \quad (6)$$

Using the upper limit of particle backscattering coefficient and the diffuse attenuation coefficient for a given chlorophyll concentration, we get the upper limit of water reflectance, $R_{lim}(545)$. The upper limit of remote sensing reflectance, can be computed using the following formula (Gordon, et. al, JGR 93, 1988):

$$Rrs_{lim}(\lambda) = (1-\rho)(1-\bar{\rho}) \cdot R_{lim}(\lambda) / (Q \cdot n^2), \quad (7)$$

where ρ is surface reflectance upwelling radiance (0.021), $\bar{\rho}$ is surface reflectance for downward irradiance(~0.043), Q is Q-factor (3.42) and n is refractive index of water (1.34).

This model limit is compared with the satellite derived remote sensing reflectance at 545nm, Rrs(545), which is the normalized water leaving radiance divided by extraterrestrial solar irradiance.

Summarizing the above description, the bit of the “turbid case 2 water” flag will be set to be 1 (on), if

$$Rrs(545) > Rrs_{lim}(545), \quad (8)$$

where $Rrs(545)$ is computed from the normalized water-leaving radiance of the pixel and $Rrs_{lim}(545)$ is computed with Eq.(7). In Eq. (7), $R_{lim}(545)$ is computed with Eq. (3) using Eqs. (4), (5) and (6).

The present algorithm for turbid water flag uses two parameters, chlorophyll concentration and normalized water leaving radiance at 545nm. It is expected that both parameters are not accurate in turbid region of interest. Conventional atmospheric correction may not give accurate result due to high value of water-leaving radiance in near-infrared bands. Chlorophyll retrieval is also difficult if case 1 water algorithm is applied. Furthermore, the radiance model and the bio-optical models that are exploited by present flag algorithm are not perfect.

Therefore, it is recommended to adjust in operation phase some of parameters in remote sensing reflectance modeling, for example, the threshold factor determining the upper limit of particle backscattering coefficient.